An Integrated Microarray Printing and Detection System to Study Protein-Protein Interactions

by

Feng Xiao

A Thesis Presented in Partial Fulfillment
of the Requirements for the Degree
Master of Science

Approved April 2017 by the
Graduate Supervisory Committee:

Nongjian Tao, Chair
Jia Guo
Chad Borges

ARIZONA STATE UNIVERSITY

May 2017

ABSTRACT

In this thesis, a breadboard Integrated Microarray Printing and Detection System (IMPDS) was proposed to address key limitations of traditional microarrays. IMPDS integrated two core components of a high-resolution surface plasmon resonance imaging (SPRi) system and a piezoelectric dispensing system that can print ultra-low volume droplets. To avoid evaporation of droplets in the microarray, a 100 μm thick oil layer (dodecane) was used to cover the chip surface. The interaction between BSA (Bovine serum albumin) and Anti-BSA was used to evaluate the capability of IMPDS. The alignment variability of printing, stability of droplets array and quantification of protein-protein interactions based on nanodroplet array were evaluated through a 10 × 10 microarray on SPR sensor chip. Binding kinetic constants obtained from IMPDS are close with results from commercial SPR setup (BI-3000), which indicates that IMPDS is capable to measure kinetic constants accurately. The IMPDS setup has following advantages: 1) nanoliter scale sample consumption, 2) high-throughput detection with real-time kinetic information for biomolecular interactions, 3) real-time information during printing and spot-on-spot detection of biomolecular interactions 4) flexible selection of probes and receptors (M × N interactions). Since IMPDS studies biomolecular interactions with low cost and high flexibility in real-time manner, it has great potential in applications such as drug discovery, food safety and disease diagnostics, etc.

DEDICATION

To my dear wife and family.

ACKNOWLEDGMENTS

I would like to thank my advisor, Dr. Nongjian Tao for his mentoring during my graduate career. Dr. Tao demonstrated me how to become a successful graduate student, which requires independent critical thinking and deep understanding for undergoing researches, encouraged me when I encountered difficulties. I have learnt not only how to research, but also how to overcome difficulties in life.

Also, I have received many helps from Dr. Shaopeng Wang. Shaopeng helped me a lot in setting up instruments and giving hints and ideas for projects. Dr. Xiaonan Shan taught me a lot of knowledge on how to conduct experiments and how to do research. Mr. Yan Wang collaborated with me for droplet project, discussions with him gave me lots of hints and ideas for this project and it was a great time to work with him. Ms. Fenni Zhang taught me on basic experimental setup. Dr. Lusheng Song helped me a lot in inspiration and discussion. Thanks Mr. Guangzhong Ma for helping me in lab. Thanks to Dr. Hui Yu and Dr. Yunze Yang for theoretical discussions.

It was a great time to work in Dr. Tao’ s group with so many talented people, I really appreciate their help from our group. I would like to thanks Dr. Limin Xiang, Ms. Yueqi Li, Ms. Yue Deng, Mr. Karan Syal, Ms. Chenwen Lin, Dr. Francis Tsow and all group members.

Finally, I would like to thank all my committee members for their valuable time and suggestions: Dr. Chad Borges, Dr. Jia Guo.

TABLE OF CONTENTS

Page

LIST OF FIGURES

CHAPTER 1

INTRODUCTION

1.1 Surface Plasmon Resonance

Surface plasmon resonance (SPR) is a resonant charge-density oscillation at the interface of two media with opposite dielectric constants excited by incident light. The charge density wave comes with an electromagnetic wave, and the field vectors can reach maxima at the interface and decay evanescently into both media. [1] Visible and infrared light is often used as incident light to excite surface plasmon due to high attenuation. Only p-polarized light (electric field is parallel to the plane of incident light beams) can excite surface plasmon on the interface between two media. When the frequency of incident light meets with the natural frequency of oscillating electrons on surface, resonance condition can be reached. The propagation constant β of surface plasmon follows the equation: $\beta = k\times(\frac{\varepsilon_m {n_s}^2}{\varepsilon_m + {n_s}^2})^{1/2}$, where ε_m is dielectric constant, and k is the free space wave number, n_s is the refractive index of the dielectric, the surface plasmon wave can be generated if the dielectric constant of interface of two media meets this equation. [2] From the equation above, silver and gold are most frequently used metals that excite surface plasmon waves. Gold is inert to biochemical reagents, therefore it is a suitable material for measuring SPR in biomolecular interactions without interference from oxidation and contaminants. Surface plasma waves could penetrate at metal-water interface for 162 nm for typical gold film under 630 nm incident light, thus, only change on the interface within the penetration depth can be detected by SPR. [3] The surface plasmon resonance angle mainly depends on the properties of metal film, the wavelength of incident light and the refractive index of

two media on the interface. [4] In the research of studying biomolecular interactions, the metal film and the incident light are fixed, target protein is modified on gold film prior to the interaction, when analyte solution of biomolecules bound with target protein on surface, refractive index of the interface changes during the process of biomolecular interactions, therefore, the characteristic resonant angle of surface plasma changes corresponding to biomolecular interactions. By measuring the change of resonance angle, the process of biomolecular interactions can be quantified. One of the most frequently used SPR configurations for practical use is Kretschmann configuration. It is an attenuated total reflection setup usually coupled with prism. In this configuration, the measurement of reflection light, resonant angle of incident light or resonant wavelength of incident light can be correlated with the process of biomolecular interactions. In Kretschmann configuration as shown in Fig. 1.1, a thin metal film covers a glass block, when light passes through this glass block, an evanescent wave penetrates through this metal film, thus plasmon can be excited on the other side of metal film. [5] Beside Kretschmann prism coupler-based configuration, there are optical waveguide based SPR, optical fiber based SPR and grating coupler-based SPR system. [1]

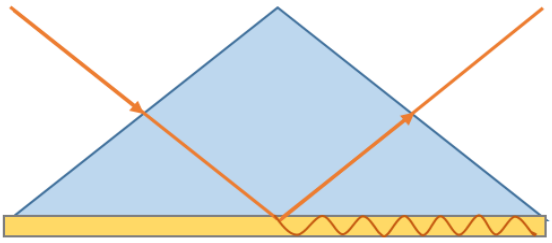

Figure 1.1 Schematic graph of Kretschmann configuration.

If the surface of gold film is coated with different biomolecules, using appropriate monochromatic light as incident light and fixed incident angle at the resonance angle, charge coupled device (CCD) camera, this technique can be extended to surface plasmon resonance imaging (SPRi). The intensity of reflection light is attenuated and a reflection spectrum is produced through absorption profile because of the energy transfer at the resonance condition. [6, 7] The refractive index change of dielectric medium varies the intensity of reflection light, therefore, it can provide high contrast images based on the adsorbed amount of molecules on sensor surface. [9-13] Intensity SPR imaging was first demonstrated by Yeatman and Ash in the late 1980s. In recent decades, numerous researches using SPRi studied interactions between epitope-antibody [14], protein-protein [15], protein-DNA [16]. It could be used for quantification and real-time monitoring of interactions between biomolecules with a direct visual view.

SPR has widely applications on the detection of interactions between biomolecules such as medical diagnostics, drug discovery, food safety and environmental monitoring. [17] Since binding of biomolecules on sensor metal chip surface can affect the refractive index of the chip, SPR signal is produced and can be used to monitor biomolecular interactions in real-time. Fig. 1.2 shows the basic principle of SPR biosensor setup: An attenuated total reflection SPR is used for measuring biomolecular interactions, an evanescent wave propagates along the interface with a propagation constant, the quantification of the binding process of analyte and surface protein is detected by the measurement of refractive index change. Biomolecular self-assemble monolayer is modified on the metal surface as probe protein, and can capture analyte (probe protein) in

liquid sample, which changes the refractive index at the metal surface. Consequently, the change of refractive index contributes to the propagation constant of surface plasmon on the metal surface. In this way, by measuring the change of intensity, angular, or wavelength of light, the change of surface plasmon can be detected, which is related to the interaction between biomolecules on chip surface. When the reflection intensity is measured as a function of incident angle, a sharp dip can be found at resonance angle. For SPR biosensors, by measuring the change of resonance dip, refractive index change can be monitored. Researches about SPR biosensor in recent years studied the interactions between biomolecules including antibodies, DNA, proteins, peptides etc. [18-25]

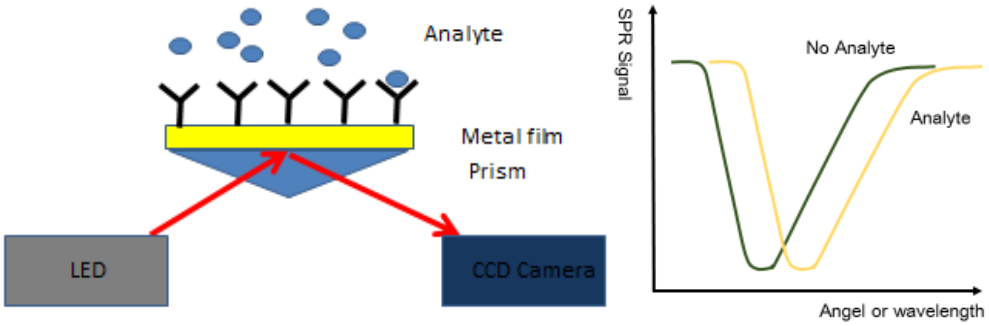

(a) (b)

Figure 1.2 Basic Principle of SPR biosensor setup. (a) Typical SPR setup for biomolecule interactions detection. (b) SPR signal shift by the binding of analyte to the surface.

1.2 Microarray

Microarray has been developed as a high-throughput method to quantify interactions between biomolecules including DNA, RNA, protein, cellular, chemicals, antibody etc. [26-29] Microarray is the chemistry on a chip, it is also called lab-on-a-chip. Chip is the core part of microarray since it is the loading surface for analytes and surface modification of target molecules. Proteinarray is the main focus of this research because protein related interactions are the main subjects of the studies in our IMPDS system. Protein-protein interactions play important role in gene expression, cell proliferation and cell growth etc. Protein can also interact with other various biomolecules such as phospholipids, small drug molecules, protein kinases et al. One of the most attractive advantages of protein array is its high-throughput detection, which enables effective and automatic detection of protein-DNA, protein-Aptamers, protein-protein, protein-RNA etc. [30-31] The two major parts of protein microarray are chips and detection. The chip for microarray is usually a glass microscope slide functionalized with a self-assembled monolayer, then protein of interest attaches to it. For the modification of protein on a chip, the goal is to immobilize protein on the surface without changing protein conformation and functionality as well as maintaining maximum bioactivity. For modification of protein on chip surface, adsorption, affinity binding and cross-linking can be used to attach protein onto surface. Cross-linking is used for more specific protein attachment. The cross-linking reagent forms a self-assembled monolayer on chip surface, the functional group on one side is used for bound with the chip, and the functional group on rear side can react with proteins, therefore, protein can be modified through covalently bond on the chip. For example, in the modification of gold chip, bifunctional thiolated-alkylene is used for cross-linking, in which thiol group reacts with gold surface and the other functional group such

as carboxylate group reacts with probe protein. [31-32] Detection part provides researchers with quantification of interactions between biomolecules as analyte and immobilized protein on the surface. Detection methods can be divided into labeling and label-free detection methods. Fluorescent, affinity, photochemical or radioisotope tags are used in protein assays as labeling methods. Fluorescence is one of the most frequently used technique because of high sensitivity and relatively simple procedures. [31, 33] Although labels can provide detection with high sensitivity, labelling itself may interfere with the bioactivity and functionality of target protein. However, label-free method can detect biomolecular interactions without interference from labels. SPR is a mature label-free technique that collects real-time kinetic data with high sensitivity and wide applicable range of molecular weights, affinities and binding constants. [34, 35] By using the technique of SPRi, Sapsford et al. developed an antibody array and achieved spots with 200 μm in diameter. [36] In conclusion, protein microarray is an extraordinary high-throughput technique that can be used to discover unknown proteins as well as studying functionality of well-studied protein-protein interactions.

1.3 IMPDS

There are several limitations of conventional SPR and microarray system. In SPR system, for conventional microfluidic SPR, the number of channels in microfluidics limits the throughput. Even for SPRi technique, global flow of analyte solution restricts kinetic analysis of one probe to N targets, which results in inflexibility of selecting desired proteins as probes. For the microarray system, spots are pre-printed blindly without any feedback on the properties of spots such as uniformity, target activity and selectivity, which is

necessary to investigate to obtain complete experimental data. For the researches on biomolecular interactions, expensive cost of purified protein is still a headache for researchers. Therefore, if there is a method with low sample consumption, the experimental cost of protein and other biomolecules can be significantly reduced for research institutes.

An integrated microarray printing and detection system (IMPDS) was proposed to solve these problems in conventional SPR and microarray. IMPDS was integrated by a high-resolution SPRi system and a piezoelectric liquid dispensing system (PLD). The target protein was printed on the surface as a high-throughput droplets array, and the probe protein was printed right onto the target protein spots. The biomolecular interactions were studied in a droplets array, the target protein and probe protein interacted within a tiny droplet on the SPR sensor chip and produced corresponding SPR signals. Firstly, since SPRi detects the SPR signal during the modification of protein, real-time information about spots during printing can be retrieved by analyzing SPRi signals. Concentration of biomolecules in spots, uniformity and geometry of spots can be studied from the start of printing, therefore, the modification process can be visualized and optimized. Moreover, the sample consumption is ultra-low because only one tiny droplet of sample solution was used for each individual interaction, and the volume for each droplet is down to few nanoliters. Comparing to sample consumption of conventional SPR with microfluidic system (several hundred microliter), the sample consumption of IMPDS is several thousand times smaller. IMPDS has unique advantage in sample consumption and therefore provide researchers with affordable cost on expensive protein, biomolecules and drugs. Furthermore, droplet-based interaction enables printing analyte protein (probe protein) on spots of modified protein (target protein) on chip, therefore, the selection of

probe protein becomes flexible and can be utilized with multiple probes onto different target protein without wasting extra probe protein. In traditional microarray techniques, probe protein is dissolved in solution and flown across whole microchip or microfluidic channel, thus only interactions between one probe and multiple targets can be detected with large amount of sample consumption for one single trial. Assuming there are N different targets on the chip, and M different probe proteins to be printed on target droplet (M and N are positive integers), then M × N interactions can be observed and detected by IMPDS platform in one experimental trial. This flexible selection of probes and targets of IMPDS enables researchers to study interactions between multiple probes to multiple targets at one time, without using numerous microarray or multiple trials of one probe to many targets.

In microarray technique, the evaporation of droplets affects the concentration of analyte and reagents so that refractive index of media and bioactivity of analyte might be changed under evaporation. At typical experimental conditions, it takes 10 to 30 s for a 10 nL drop to evaporate. [37] Since SPR signal is directly related to refractive index change, it is crucial to deal with evaporation issue in IMPDS. Evaporation can be reduced by several methods: continuous adding liquid to reservoir, blocking the gas-liquid interface by mineral oil or heptane and increasing humidity in environment. [38-41] By using these methods to manage evaporation of droplets, droplet-based array can be stable enough for measuring biomolecular interactions.

Overall, IMPDS integrated a SPRi system and a piezoelectric liquid dispenser to achieve printing with high accuracy and detection of protein-protein interactions and other biomolecular interactions. Comparing to traditional SPR and microarray system, IMPDS

is a label-free method with ultra-low sample consumption (nanoliter scale), high resolution, high throughput and flexible selection of probe and target proteins (M × N interactions), which renders it huge potential for further application to study biomolecular interactions in drug discovery, disease diagnostics, food safety, etc.

CHAPTER 2

EXPERIMENTAL

2.1 *Materials*

Phosphate-buffered saline (PBS, pH = 7.4) was purchased from Cellgro (Corning Inc., NY, USA), dithiolalkanearomaticPEG6-COOH (Dithiol-PEG-COOH) and dithiolalkanearomaticPEG3-OH (Dithiol-PEG-OH) were purchased from SensoPath Technologies (Bozeman, MT), 1-ethyl-3-(3-dimethylaminopropyl)carbodiimide hydrochloride (EDC• HCl) was purchased from Thermo Fisher (Waltham, MA), sodium acetate (NaAc), N-Hydroxy-succinimide (NHS), ethanolamine (EA), dedocane, Albumin from bovine serum (BSA) and anti-BSA(B1520) were purchased from Sigma-Aldrich(St. Louis, MO), immersion oil(Type NVH) was purchased from Cargille (Cedar Grove, NJ).

2.2 IMPDS Setup

A distortion-free prism based SPRi detector was integrated with an ultra-low volume piezoelectric microarray printer. The SPRi detector consists of a point source LED light, collimation lens with tunable incident angle (Thorlabs), a SF11 prism (Dow Corning), 12× variable zoom lens (Thorlabs) and a USB3 CMOS camera (FLIR FL3-U3-13Y3M-C). The SPRi detector was inserted between the bottom supporting base and the top deck of the printer using a customized designed metal frame.

The components on the printing deck were rearranged to accommodate the SPRi detector including: microplate used as solution reservoir, side-view video camera, wash

station and ultrasonic cleaner. The breadboard version IMPDS setup dispensed from the printhead and nanodroplets fell onto the microchip. Software for both the SPRi detector and the microarray printer were integrated into a single Windows 7 computer.

2.3 Printing Capability and Alignment Variability Analysis

Four nozzles of different sizes were used, the diameters of nozzles are 22, 49, 67, 75 μm respectively. The alignment variability is characterized by comparing the distance between the center of first printing and the center of second printing in a 10 x 10 microarray. A customized Matlab program was written to process microarray images in order to quantify alignment variability. The relative alignment variability is defined as the standard deviation of the ratio of center-to-center displacement of all droplets divided by diameters of all droplets.

2.4 Evaporation Control

A novel technique was developed to maintain nanodroplet stability at room temperature. A thin layer of oil was used to cover the surface of microchip in order to eliminate droplet evaporation. Before printing nanodroplets on the chip, 50 μl dodecane ($C_{12}H_{26}$) oil was pipetted onto the gold chip as SPR sensor, then oil spread out across the gold chip to form a uniform layer with a thickness of about 100 μm. After that, droplets dispensed from printhead penetrated through the oil layer, displaced the oil and adhered to

the gold chip surface due to surface tension and gravity. Evaporation test was done by comparing the change of SPR intensity of droplets with and without oil covering.

2.5 Modification of Bovine Serum Albumin(BSA)

The SPR sensor chips were BK-7 glass coverslips coated with 2 nm thick of chromium then followed with 47 nm thick of gold. Before surface functionalization, sensor chips were rinsed by deionized water and ethanol, blown to dry with nitrogen, and cleaned by hydrogen flame. Then cleaned chips were incubated overnight in 1 mM mixed dithiol solution containing 10:1 dithiol-PEG-OH/dithiol-PEG-COOH in ethanol. The chip was placed on prism with one drop of immersion oil. A solution of 0.4 M EDC and 0.1 M NHS in deionized water was freshly prepared and then deposited onto the chip to activate the surface. After 15 min, the chips were thoroughly cleaned by deionized water, covered by 100 μm oil and then 4 nL of 200 μg/ml BSA dissolved in NaAc (pH = 5.3) was printed onto the chip surface and allow the protein to adequately bind with modified surface. SPR signal of BSA binding was recorded until modification of BSA reached equilibrium.

2.6 Washing Excess BSA and Blocking

The chip was washed with 1X PBS buffer several times to remove excess BSA on each spot and oil. After washing, 1M ethanolamine was used to block the surface for 15 minutes. The chip was washed again by 1X PBS and then washed with deionized water to remove blocking reagent and buffer residue on the surface. Finally, the chip was dried in

air and prepared for analyte printing. SPR signal of blocking was recorded until blocking reached equilibrium.

2.7 Analyte Printing

A 100 μm thick oil layer was used to cover the chip. After depositing new oil layer on the chip, print an array of 1X PBS buffer spots to collect baseline, and then print different concentrations of Anti-BSA as droplets on the surface at the same location as spots in the modification of BSA. SPR signal on each spot was recorded until binding reached equilibrium.

2.8 Dissociation

1X PBS buffer was flown through chip surface with a flow rate of 500 μL/ min by a gravity-based drug perfusion system (SF-77B, Warner Instruments, CT), washing away anti-BSA droplets as well as oil layer. SPR signal on each spot was recorded for 30 minutes for dissociation.

2.9 Conventional SPRi Experiment

To validate and compare the kinetics constants obtained from IMPDS measurement, a BI-3000 system (Biosensing Instrument), a commercialized SPR setup, was used to measure binding kinetic constants of BSA to Anti-BSA.

CHAPTER 3

RESULTS AND DISCUSSION

3.1 Breadboard Version of IMPDS

A breadboard version of IMPDS system was developed as shown in Fig. 3.1. A piezoelectric liquid dispensing (PLD) system was integrated with a high-resolution surface plasmon resonance imaging(SPRi) system. The PLD can print single droplet of less than 0.1 nL and the SPRi can display high-resolution surface plasma resonance images with a noise level less than 1 Response Unit (RU).

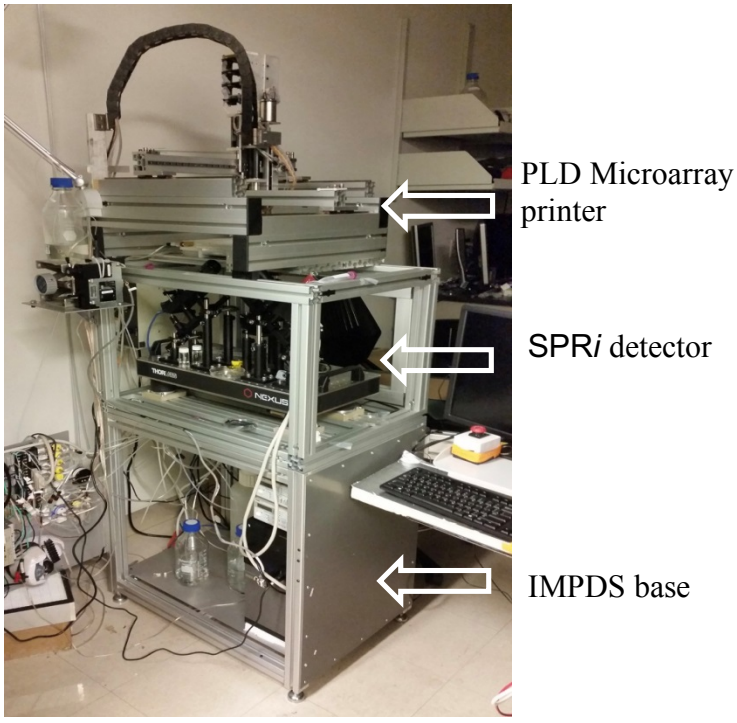

Figure 3.1 The breadboard version of IMPDS.

3.2 Printing Capability of Piezoelectric Liquid Dispensing System

Nanodroplets were dispensed from the piezoelectric liquid dispensing system, which is the printer in IMPDS. Droplets were dispensed with a speed from 0.5 to 10 mm/s at print-head. With different sizes of nozzles, the volume of each drop is in the range of 0.1 nL to 0.6 nL and the frequencies of drops were from 5,000 to 24,000 drops-per-second. The PLD can adjust the volume of each spot by controlling the number of drops dispensed at each spot from one to several hundred drops per spot.

In order to demonstrate the concept of kinetic measurement in droplets, the alignment of droplets has to be taken into account. To verify alignment variability, a 10 × 10 array were printed onto a gold chip twice at the same location, with a 0.8 mm spacing between spots and a volume of 3 nL for each spot. The distance between the center of each spot for first time print and the center of each spot for second time print was calculated. Thus, alignment variability was characterized by comparing the standard deviation of center-to-center displacement between two prints with the diameter of each spot. This 10 × 10 nanodroplet microarray and the result of its alignment variability are shown in Fig. 3.2. The standard deviation of center-to-center displacement between the two prints is d = 12.4 μm, and the average diameter of droplet is D = 375.6 μm. The relative alignment variability is defined as d/D, which is 3.3% on average. Thus, IMPDS shows capabilities of adjusting printing volume and speed for each droplet with accurately printing, which renders IMPDS huge potential for accommodating requirements in terms of physical properties of droplets in future researches.

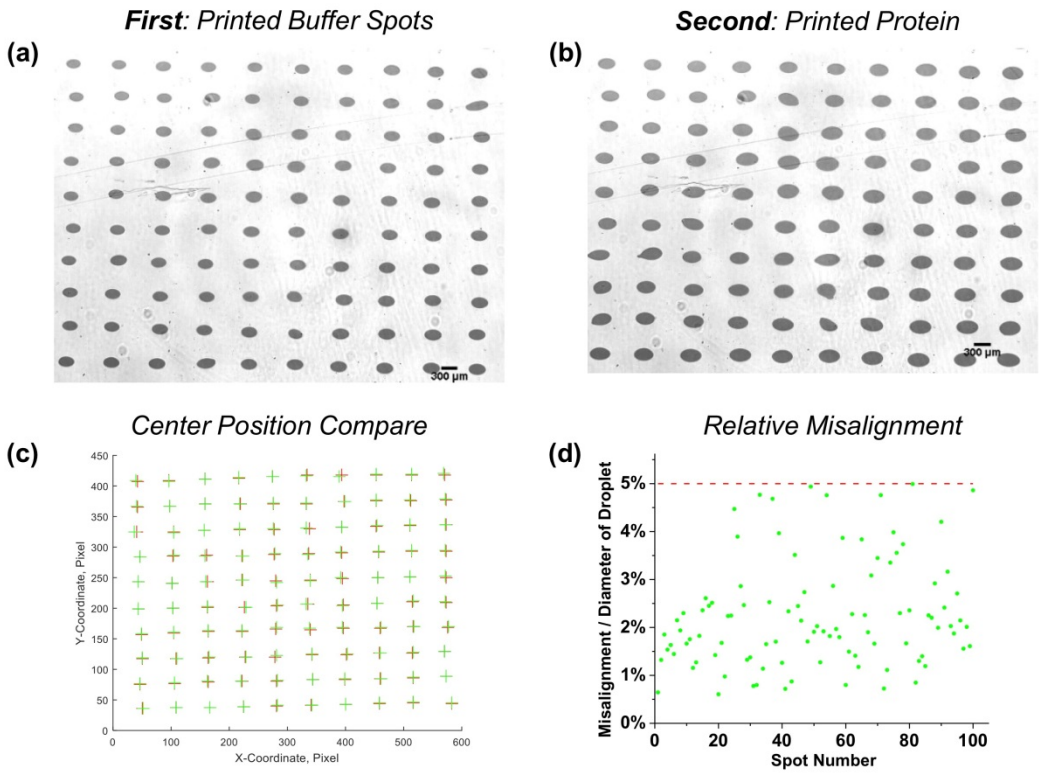

Figure 3.2 Alignment variability of IMPDS. (a) SPR image of a 10 × 10 spot microarray after first print, spot volume 3 nL. (b) SPR image of the 10 × 10 nanodroplet microarray after spot-on-spot second print of 3nL liquid on the same location as first print. (c) The center position of the droplets: red crosses are centers of the first droplet, and green crosses are centers of spot after second print. (d) Relative alignment variability of the individual spots calculated by dividing the displacement distance, d, between the two prints by the final spot diameter, D.

3.3 Nanodroplets Stability against Evaporation

Evaporation often has serious negative effects on microarray performance such as data quality and reproducibility, which is even worse with smaller volume of droplets. In order

to eliminate evaporation in IMPDS, an oil layer of dedocane was deposited on the sensor chip before printing and then dispensed droplets penetrated the oil layer and adhered to the chip. The oil layer blocked the interface between air and aqueous droplets, therefore, the evaporation of nanodroplets can be minimized. Fig. 3.3a demonstrates a schematic setup of oil layer and droplets array, and Fig. 3.3b shows an image of top view of a 10×10 microarray under oil layer. There was an obvious difference in SPR response between droplets in air and droplets in oil, and the result is shown in Fig. 3.3c. The SPR signal of a droplet in oil stays flat over time indicating that no observable evaporation during 10 minutes assay time, while the SPR signal of the droplet in air increased rapidly two minutes after printing, resulting from evaporation induced refractive index change. In addition, the oil cover layer does not contribute to the SPRi response of the droplet, because SPR is only sensitive to the refractive index changes within a few hundred nanometers near the surface, and the droplets are several tens of micrometers high.

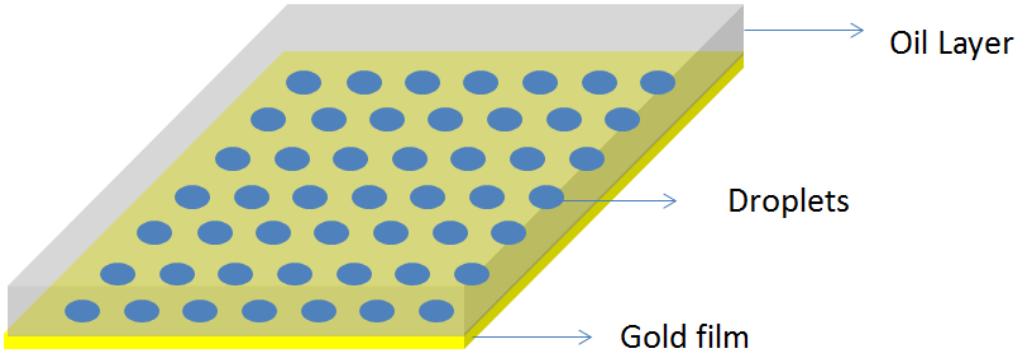

(a)

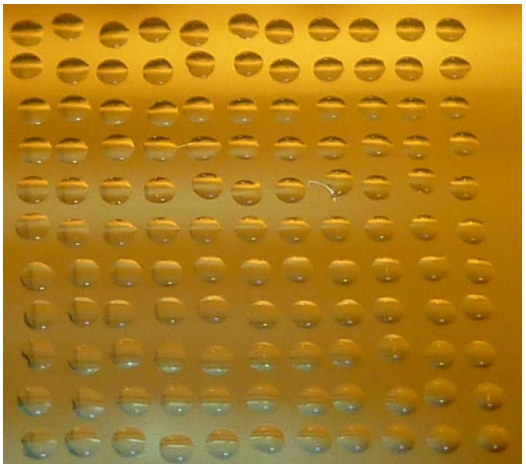

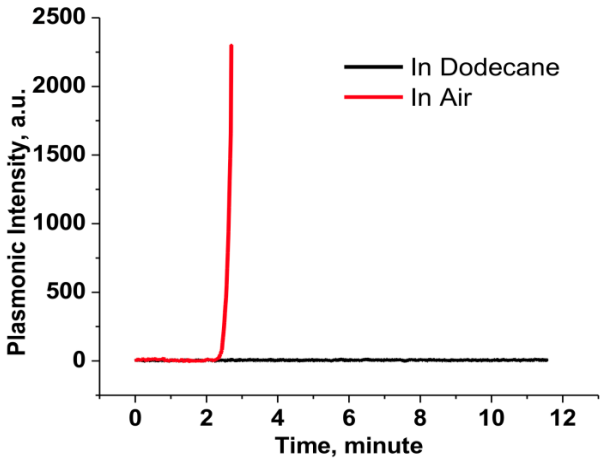

(b) **(c)**

Figure 3.3 Nanodroplets against Evaporation. (a) Schematic graph of the oil layer setup on sensor chip. (b) Image of top view of microchip with a 10 × 10 microdroplets array and dedocane layer on surface. (c) SPR response for a droplet of PBS buffer in air and in dodecane.

3.4 Quantification of Protein-binding Interactions for a Drop-on-drop Based Assay

IMPDS system enables real-time measurement of protein-protein interactions in microdroplets. Droplet-based measurement significantly reduces sample consumption from microliter scale into nanoliter scale. Multiple binding pairs can be measured simultaneously on the same sensor chip by IMPDS. In conventional SPR setup, the concentration of analyte is considered as a constant because of continuous flow of analyte solution in microchannels. However, the amount of analyte in droplet-based protein-protein interactions is limited and depleted over the binding process. Also, diffusion process of analyte should be taken into account for a complete model that evaluates binding kinetics in droplet-based array. Therefore, it is necessary to consider the effects of depletion and diffusion in order to obtain accurate kinetic information for association process.

COMSOL Multiphysics was used to simulate the effects of diffusion and depletion in droplets. The geometry of droplet is semi-ellipsoid, the diameter and height of the droplet is 200 μm and 80 μm respectively, diffusion coefficient as 4.7×10^{-10} m^2/s, initial concentration of analyte was 50 nM and surface concentration of BSA is 1.49×10^{-14} mol/mm^2. The simulation results were shown in Fig. 3.4. the concentration of analyte shows distribution across the droplet after 100 s, most of the analyte were reacted with protein modified on surface and depleted after 900 s in the simulation. Thus, it is necessary to analyze the process of protein-protein interactions with a new model in order to apply kinetic analysis in droplet-based array.

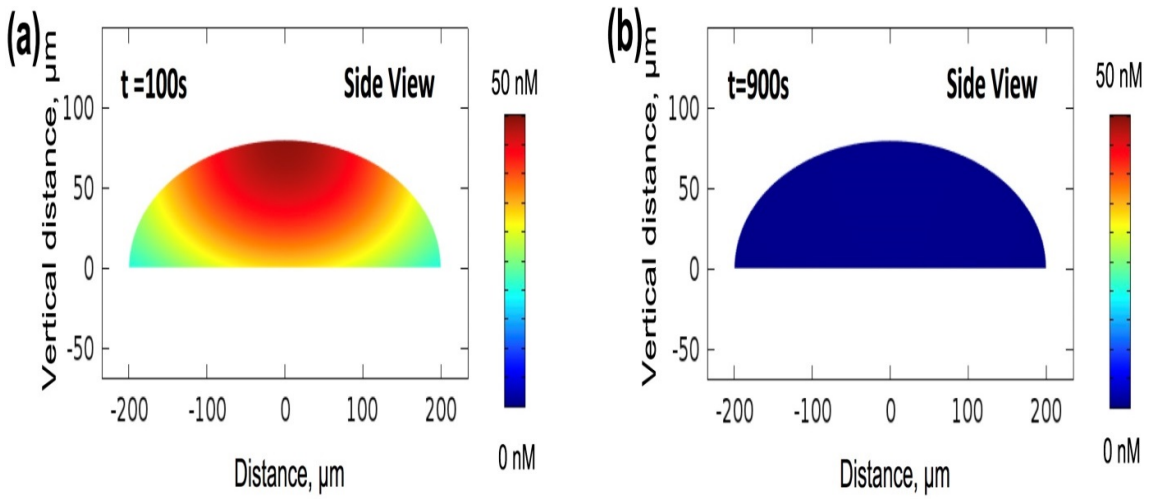

Figure 3.4 Simulation results of concentration distribution in a droplet with a radius of 200 μm at two different binding times.

To analyze the binding kinetics in the droplet, we built a new model that takes both of diffusion and depletion into account. The interaction between surface modified protein and analyte is described as following equation:

$$\frac{\partial C_{AB}(t)}{\partial t} = k_a C_A(0,t)(C_B(0) - C_{AB}(t)) - k_d C_{AB}(t), \quad (1)$$

Where C_A, C_B and C_{AB} is the volume concentration of the analyte in the droplet, the surface concentrations of the receptor protein and the bound product on the sensor surface, respectively. $C_A(z,t)$ indicates the concentration of analyte at height of z μm and k_a and k_d are association and the dissociation rate constant, respectively. The measured SPR signal is scaled with the surface concentration of bound product at specific angle:

$$\Delta\theta = \alpha C_{ab} \quad (2)$$

where α is a constant.

The diffusion of analyte from bulk to the surface follows:

$$\frac{\partial C_A(z,t)}{\partial t} + \nabla \cdot \left(D \frac{\partial C_A(z,t)}{\partial z} \right) = R_i, \quad (3)$$

where D is the diffusion constant, z is distance to the sensor surface and t is time, and

$$R_i = \begin{cases} 0, & z > 0 \\ \dfrac{\partial C_A(0,t)}{\partial t} (Obtain\ from\ Eq.1), & z = 0' \end{cases} \quad (4)$$

The depletion of analyte is included in the boundary conditions:

$$\int C_A(z,t)\, S dz = C_{A0} V - C_{AB}(t) S, \quad (5)$$

where V and S is the volume and surface area of the droplets, respectively. As shown in Fig. 3.5, this model of the association process fits the experimental data very well.

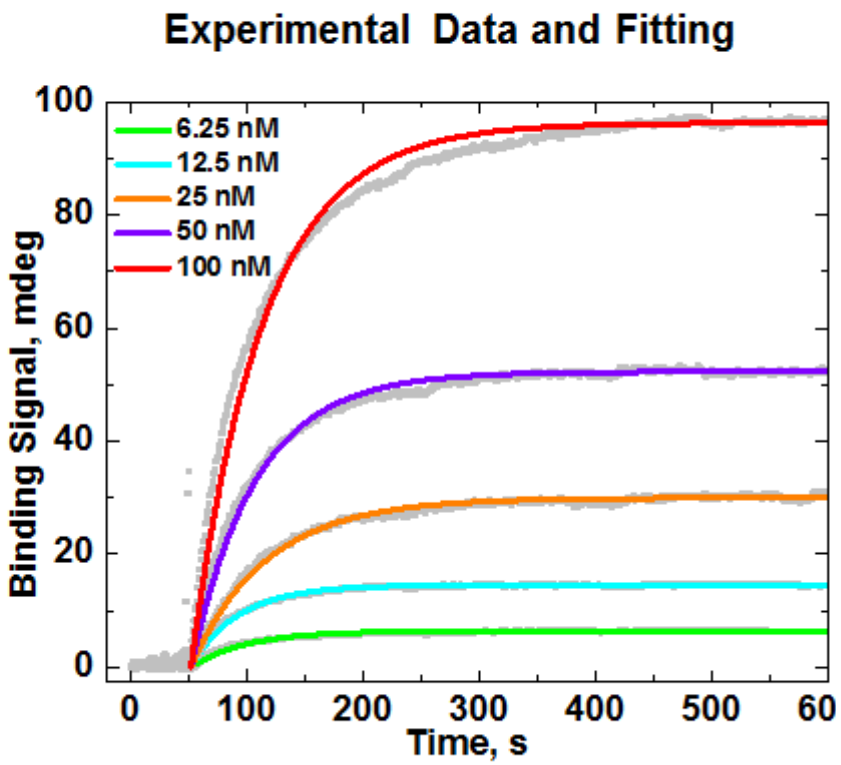

Figure 3.5 IMPDS data (grey colored curves) between different concentrations of anti-BSA binding to surface modified BSA fitted by the analytical model we built. The green, cyan, orange, violet and red curve are the fitted curves of binding 6.25 nM, 12.5 nM, 25 nM, 50 nM and 100 nM anti-BSA binding signal.

3.5 Sensitivity Analysis

Signal-to-noise ratio (SNR) is characterized by quantifying standard deviation of signal in a short time on IMPDS setup. As shown in Fig. 3.6, the fluctuation of SPRi signal for 30 seconds was recorded, which describes the noise level of IMPDS system. The noise

level is 0.26 RU according to the standard deviation of intensity fluctuation. As detection limit is three times of noise level, the detection limit of IMPDS is 0.78 RU.

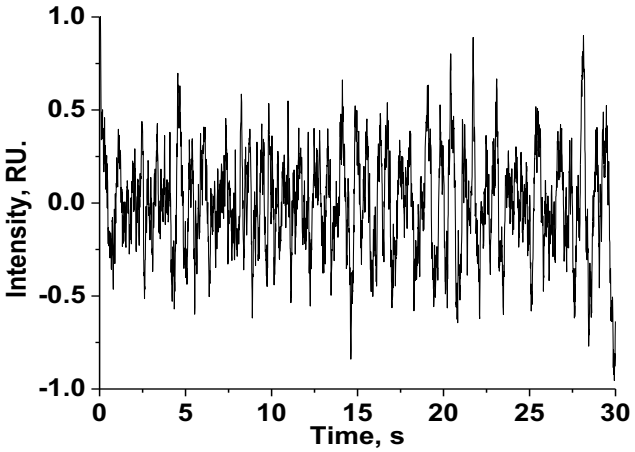

Figure 3.6. Noise levels of the breadboard IMPDS setup, the standard deviation of the plot is 0.26 RU.

3.6 Evaluating Binding Kinetic Constants in Droplet-based Array

For microarray technology, the uniformity of measurements among spots is an important factor to evaluate the quality of the technique. To quantify spot to spot variation of the IMPDS system, we measured a 10 × 10 array of anti-BSA antibody binding to BSA (Bovine serum albumin) functionalized spots. As demonstrated in Fig. 3.7, the experimental process is shown as a flow chart dividing into four major steps: 1) Preparation and calibration of the sensor chip, 2) Modification of receptor protein (BSA) on the sensor chip surface, 3) Measurement of the protein-protein interaction, 4) Process the data to

obtain the association constant, dissociation constant and equilibrium constant of each spot. Further details of procedures in each step was listed in Fig. 3.7.

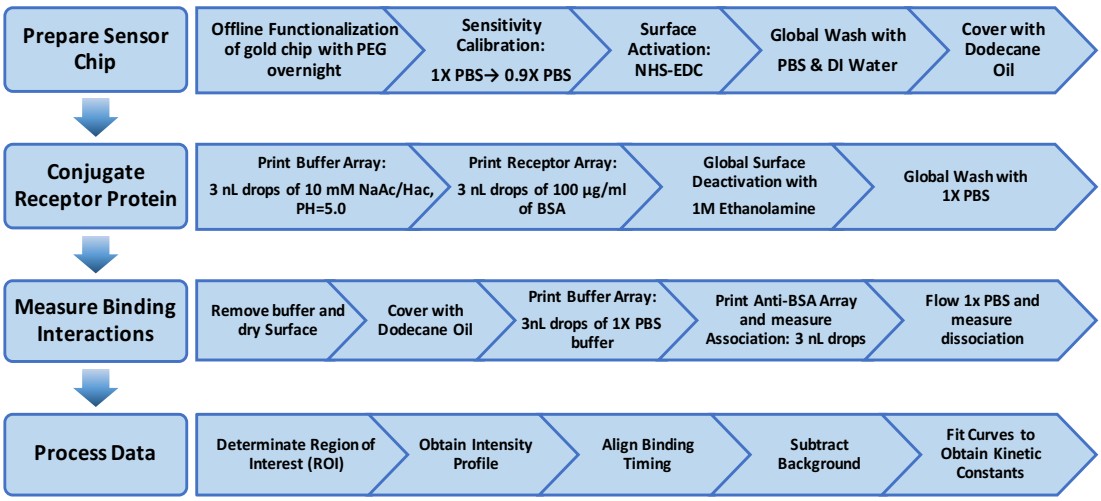

Figure 3.7 Flow chart illustrates a typical IMPDS experimental process.

3.7 Modification of Receptor Protein:

Fig. 3.8(a) shows the relative sensitivity of 100 spots during calibration by changing from 1X PBS buffer to 0.9X PBS buffer. Fig. 3.8(b) shows the SPR response of each spot in the process of modification of 6 nL 200 µg/mL receptor protein (BSA) to the sensor surface. The amplitude variation of BSA binding signal on different spots could be resulted from multiple reasons: variation in droplet volumes, droplet to surface contact angles and binding efficiency etc. However, this variation does not affect the measurement of binding kinetics, as discussed in later section. Fig. 3.8(c) is the differential SPR image showing the BSA binding after reaching equilibrium. This image was obtained by subtracting the image

of equilibrium of BSA modification from the image of 10 × 10 array of buffer, from this image, the spots is brighter than background, which indicates receptor protein BSA is modified on chip.

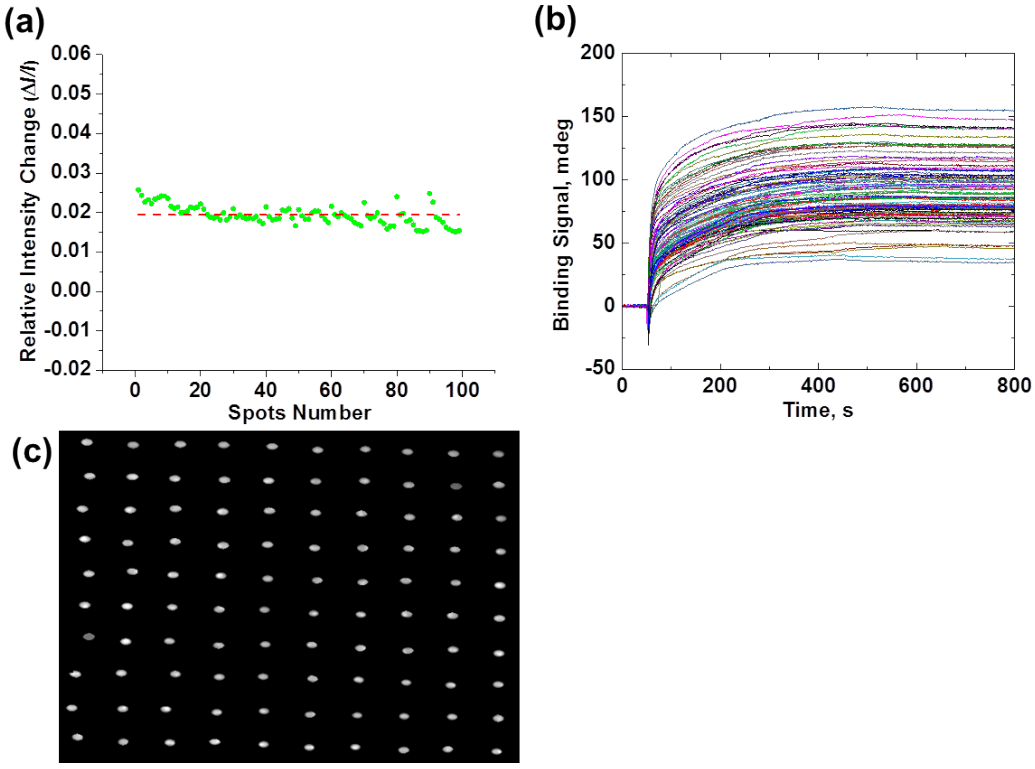

Figure 3.8 (a) Relative Intensity change during calibration; (b) Plasmonic Response of BSA modification; (c) Differential SPR image shows the BSA binding signals of the 10 x 10 spots.

3.8 Measurement of Kinetic Process

After modification of BSA on all spots, 6 nL droplets of analyte molecules (anti-BSA antibody) with 5 different concentrations (6.25 nM, 12.5 nM, 25 nM, 50 nM, 100 nM) were dispensed onto the BSA spots with two row replicates for each concentration. Fig. 3.9(a)

shows the differential SPR image that reflects the maximum anti-BSA binding at each spot, obtained by subtracting the SPR image recorded at 600s (maximum anti-BSA binding) from the SPR image recorded right before printing the anti-BSA droplets (50s). It is obvious that analyte of higher concentration of anti-BSA generates brighter spots, which means more binding interactions occured on spots with higher concentration. After association, the dissociation process was measured by continuously flowing 1X PBS globally on chip surface. Fig. 3.9(b) is the averaged association and dissociation curves curve for each concentration.

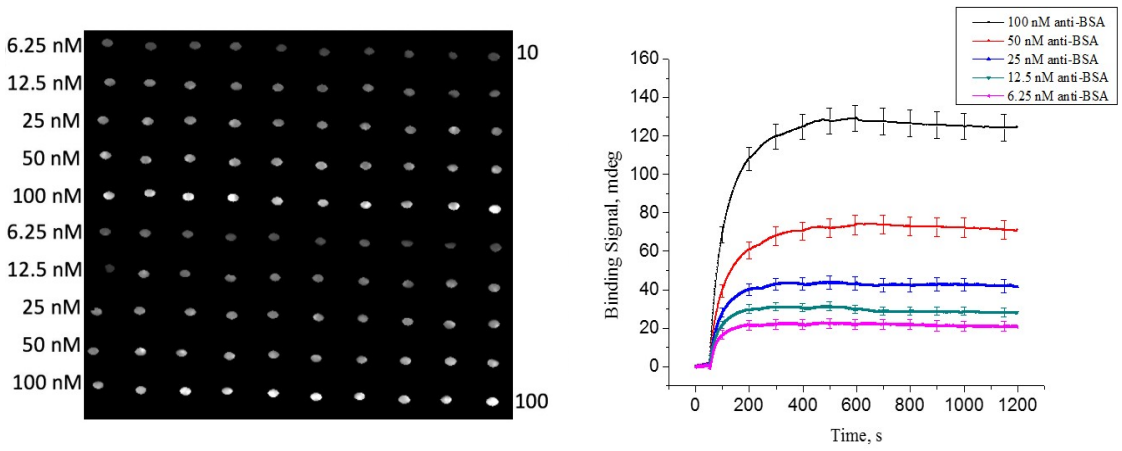

(a) (b)

Figure 3.9 (a) Differential SPR image of anti-BSA binding. Left concentrations indicate different concentrations of anti-BSA used, and numbers on the right indicates the counting manner for this droplet-based array. (b) SPR curves of association and dissociation for 5 concentrations after average, association starts from 50 s to 600 s, and dissociation occurs after 600 s.

3.9 Calculation of Kinetic Constants

The association rate constant k_a, dissociation rate constant k_d, and equilibrium constant K_D, were obtained by using new model to fit the experimental data. Fig. 3.10 shows the histogram of the kinetic constants of the 100 spots. The average values for k_a, k_d and K_D are $8.2 \pm 0.1 \times 10^4$ $M^{-1}s^{-1}$, $3.7 \pm 0.1 \times 10^{-5}$ s^{-1} and $4.5 \pm 0.1 \times 10^{-1}$ nM, respectively. The relative variation of the rate constants and binding affinity is within ±5%. To validate the kinetic results, kinetic constants of same sample was measured by a commercial SPR instrument BI-3000, and the measured kinetic constants are $k_a = 8.5 \pm 0.1 \times 10^4$ $M^{-1}s^{-1}$, $k_d = 4.9 \pm 0.2$

$\times 10^{-5}$ s^{-1} and $K_D = 5.8 \pm 0.2 \times 10^{-1}$ nM, respectively. Therefore, results from IMPDS closely match results from commercial SPR setup, which indicates that IMPDS can measure kinetic constants accurately.

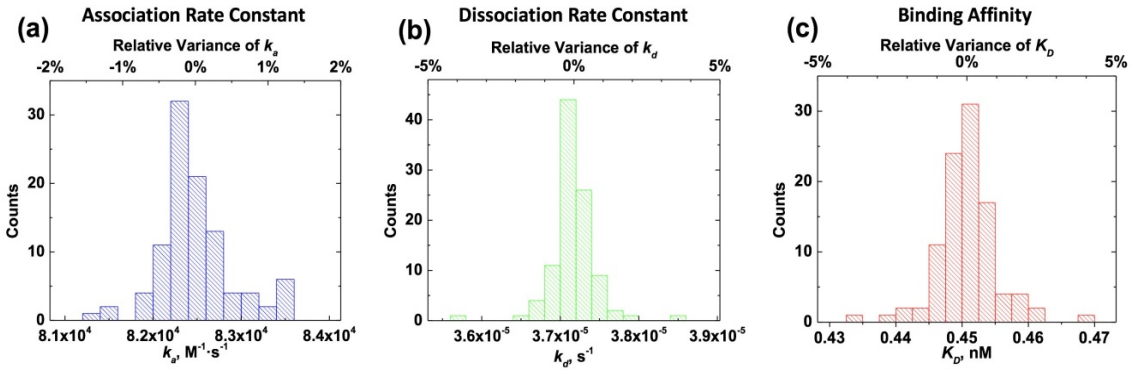

Figure 3.10 (a), (b) and (c) are histogram of k_a, k_d and K_D of 10 × 10 spots respectively.

3.10 Analysis of the Relationship between Binding Signal and Kinetic Constant

The intensity of SPR signal shows some variations among the spots, therefore, it is necessary to evaluate the impact of variation of signal intensity on the kinetic calculation. Pearson correlation was used in this evaluation. Correlation maps were plotted as in Fig. 3.11. From correlation maps, since correlation coefficients in these maps are small and p-values are larger than 0.05, correlations between the concentration of protein and kinetic constants are very weak and not statistically significant. Therefore, variations in signal intensity of different spots are very weakly correlated with binding kinetic constants in our model, which means that these variations have no impact in evaluating three binding kinetic constants.

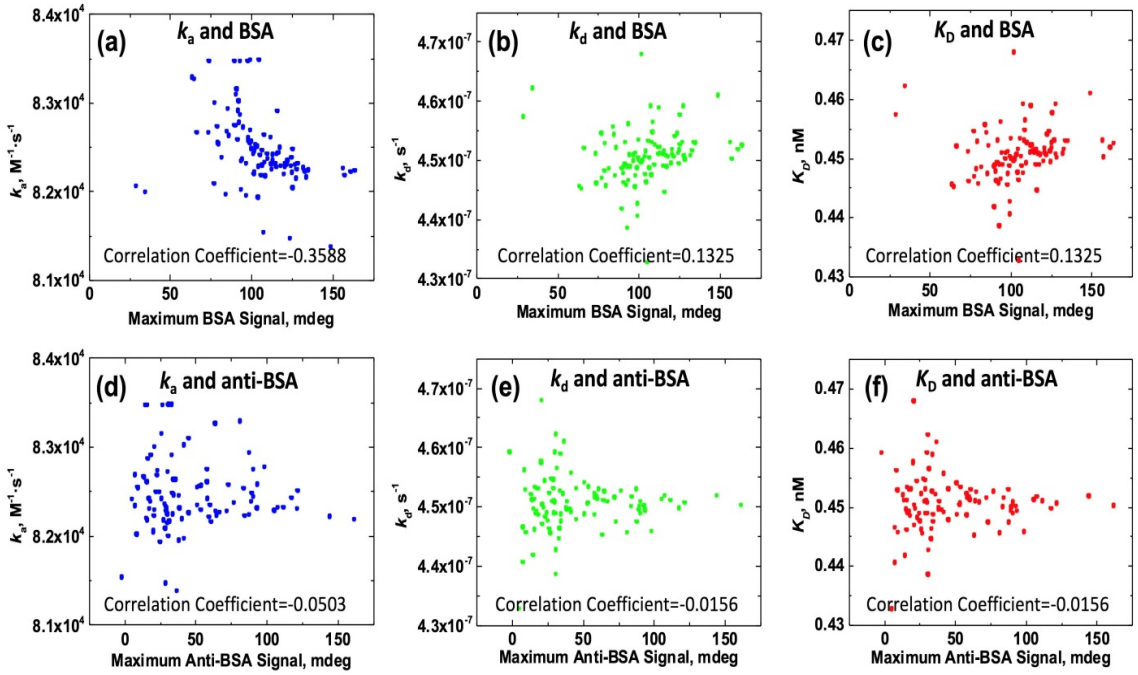

Figure 3.11 Correlation maps between binding kinetic constants and maximum binding signals among the 100 spots. P-values for correlation from (a) to (f) are 0.0798, 0.7333, 0.8089, 0.1015, 0.8847, 0.4195, respectively.

CHAPTER 4

CONCLUSIONS

In this thesis, Evaporation of droplets was managed by depositing an oil layer on chip surface. The capability of printer and alignment of droplet-based microarray were studied. A new model considering depletion and diffusion was introduced for droplet-based biomolecular interactions. Kinetic measurement of interaction between BSA and Anti-BSA was successful in a 10 × 10 microarray by IMPDS. After fitting experimental data with new model, kinetic constants including k_a, k_d, K_D for the interaction are close to commercialized SPR setup, which indicates the capability of IMPDS to measure biomolecular interactions with accurate kinetic information. Owning to ultra-low sample consumption, flexible selection of probe and target proteins and real-time monitoring on droplet-based array, IMPDS is a high-throughput method that can study biomolecular interactions with very low cost of biomolecules and investigate multiple interactions at the same time.

REFERENCES

[1] Homola, Jiří, Sinclair S. Yee, and Günter Gauglitz. "Surface plasmon resonance sensors: review." *Sensors and Actuators B: Chemical* 54.1 (1999): 3-15.

[2] Raether, Heinz. " Surface plasmons on smooth surfaces. " *Springer Berlin Heidelberg*, 1988.

[3] Ordal, M. A., et al. "Optical properties of the metals al, co, cu, au, fe, pb, ni, pd, pt, ag, ti, and w in the infrared and far infrared." *Applied Optics* 22.7 (1983): 1099-1119.

[4] Biacore AB BIACORE Technology Handbook. (1998).

[5] Kretschmann, Erwin, and Heinz Raether. "Notizen: radiative decay of non radiative surface plasmons excited by light." *Zeitschrift für Naturforschung A* 23.12 (1968): 2135-2136.

[6] Homola, Jiří. "Present and future of surface plasmon resonance biosensors." *Analytical and bioanalytical chemistry* 377.3 (2003): 528-539.

[7] Wong, Chi Lok, and Malini Olivo. "Surface plasmon resonance imaging sensors: a review." *Plasmonics* 9.4 (2014): 809-824.

[8] Piliarik, Marek, and Jiří Homola. "SPR sensor instrumentation." *Surface Plasmon Resonance Based Sensors* (2006): 95-116.

[9] Jordan, Claire E., et al. "Surface plasmon resonance imaging measurements of DNA hybridization adsorption and streptavidin/DNA multilayer formation at chemically modified gold surfaces." *Analytical Chemistry* 69.24 (1997): 4939-4947.

[10] Jordan, Claire E., and Robert M. Corn. "Surface plasmon resonance imaging measurements of electrostatic biopolymer adsorption onto chemically modified gold surfaces." *Analytical chemistry* 69.7 (1997): 1449-1456.

[11] Nelson, Bryce P., et al. "Near-infrared surface plasmon resonance measurements of ultrathin films. 1. Angle shift and SPR imaging experiments." *Analytical chemistry* 71.18 (1999): 3928-3934.

[12] Nelson, Bryce P., et al. "Surface plasmon resonance imaging measurements of DNA and RNA hybridization adsorption onto DNA microarrays." *Analytical chemistry* 73.1 (2001): 1-7.

[13] Wong, Chi Lok, George Chen, and Beng Koon Ng. "Two-dimensional surface plasmon resonance (SPR) biosensor based on infrared imaging." *Optical Molecular Probes, Imaging and Drug Delivery*. Optical Society of America, 2011.

[14] E. Yeatman and E. A. Ash, “Surface plasmon microscopy,” Electron. Lett. 23, 1091–1092 1987.

[15] Smith, Emily A., et al. "Surface plasmon resonance imaging studies of protein-carbohydrate interactions." *Journal of the American Chemical Society* 125.20 (2003): 6140-6148.

[16] Wegner, Greta J., et al. "Fabrication of histidine-tagged fusion protein arrays for surface plasmon resonance imaging studies of protein− protein and protein− DNA interactions." *Analytical chemistry* 75.18 (2003): 4740-4746.

[17] Wong, Chi Lok, and Malini Olivo. "Surface plasmon resonance imaging sensors: a review." *Plasmonics* 9.4 (2014): 809-824.

[18] Wilson, S., and S. Howell. "High-throughput screening in the diagnostics industry." (2002): 794-797.

[19] Van Regenmortel, M. H. "Use of biosensors to characterize recombinant proteins." *Developments in biological standardization* 83 (1993): 143-151.

[20] Tsurumi, Yoshiaki, et al. "Production of antibody against a synthetic peptide of Porphyromonas gingivalis 40-kDa outer membrane protein." *Journal of oral science* 45.2 (2003): 111-116.

[21] Park, Junguk, Hua Fu, and Dehua Pei. "Peptidyl aldehydes as reversible covalent inhibitors of Src homology 2 domains." *Biochemistry* 42.17 (2003): 5159-5167.

[22] Nguyen, Binh, et al. "Influence of compound structure on affinity, sequence selectivity, and mode of binding to DNA for unfused aromatic dications related to furamidine." *Biopolymers* 63.5 (2002): 281-297.

[23] Rich, Rebecca L., et al. "High-resolution and high-throughput protocols for measuring drug/human serum albumin interactions using BIACORE." *Analytical biochemistry* 296.2 (2001): 197-207.

[24] Thorpe, Robin, and Steven J. Swanson. "Current methods for detecting antibodies against erythropoietin and other recombinant proteins." *Clinical and diagnostic laboratory immunology* 12.1 (2005): 28-39.

[25] Van Regenmortel, M. H. "Use of biosensors to characterize recombinant proteins." *Developments in biological standardization* 83 (1993): 143-151.

[26] Seidel, Michael, and Reinhard Niessner. "Automated analytical microarrays: a critical review." *Analytical and bioanalytical chemistry* 391.5 (2008): 1521.

[27] Fodor, Stephen PA, et al. "Light-directed, spatially addressable parallel chemical synthesis." *science* (1991): 767-773.

[28] Angenendt, Philipp. "Progress in protein and antibody microarray technology." *Drug discovery today* 10.7 (2005): 503-511.

[29] Cretich, Marina, et al. "Protein and peptide arrays: recent trends and new directions." *Biomolecular engineering* 23.2 (2006): 77-88.

[30] Green, Louis S., Carol Bell, and Nebojsa Janjic. "Aptamers as reagents for high-throughput screening." *Biotechniques* 30.5 (2001): 1094-100.

[31] Templin, Markus F., et al. "Protein microarray technology." Drug discovery today 7.15 (2002): 815-822.

[32] Houseman, Benjamin T., et al. "Peptide chips for the quantitative evaluation of protein kinase activity." *Nature biotechnology* 20.3 (2002): 270-274.

[33] Haab, B. B. "Advances in protein microarray technology for protein expression and interaction profiling." *Current opinion in drug discovery & development* 4.1 (2001): 116-123.

[34] McDonnell, James M. "Surface plasmon resonance: towards an understanding of the mechanisms of biological molecular recognition." *Current opinion in chemical biology* 5.5 (2001): 572-577.

[35] Salamon, Zdzislaw, Michael F. Brown, and Gordon Tollin. "Plasmon resonance spectroscopy: probing molecular interactions within membranes." *Trends in biochemical sciences* 24.6 (1999): 213-219.

[36] Sapsford, Kim E., et al. "Kinetics of antigen binding to arrays of antibodies in different sized spots." *Analytical chemistry* 73.22 (2001): 5518-5524.

[37] Jackman, Rebecca J., et al. "Fabricating large arrays of microwells with arbitrary dimensions and filling them using discontinuous dewetting." *ANALYTICAL CHEMISTRY-WASHINGTON DC-* 70 (1998): 2280-2287.

[38] Berthier, Erwin, et al. "Managing evaporation for more robust microscale assays Part 1. Volume loss in high throughput assays." *Lab on a Chip* 8.6 (2008): 852-859.

[39] Bratten, Craig DT, Peter H. Cobbold, and Jonathan M. Cooper. "Micromachining sensors for electrochemical measurement in subnanoliter volumes." *Analytical Chemistry* 69.2 (1997): 253-258.

[40] Litborn, Erik, and Johan Roeraade. "Liquid lid for biochemical reactions in chip-based nanovials." *Journal of Chromatography B: Biomedical Sciences and Applications* 745.1 (2000): 137-147.

[41] Clark, Rose A., Paula Beyer Hietpas, and Andrew G. Ewing. "Electrochemical analysis in picoliter microvials." *Analytical Chemistry* 69.2 (1997): 259-263.